

Quantifying intra-urban morphology of the Greater Dublin area with spatial metrics derived from medium resolution remote sensing data

Tim Van de Voorde, Frank Canters

Cartography and GIS Research Group, Dept. of Geography
Vrije Universiteit Brussel
Brussels, Belgium
tim.vandevoorde@vub.ac.be

Johannes van der Kwast, Guy Engelen

Flemish Institute for Technological Research (VITO)
Mol, Belgium
hans.vanderkwast@vito.be

Marc Binard, Yves Cornet

Unité de Géomatique, Dept. of Geography,
Université de Liège
marc.binard@ulg.ac.be

Abstract—Spatial metrics derived from satellite imagery are useful measures to quantify structural characteristics of expanding cities, and can provide indications of functional land use types. Images of medium resolution are cheap, widely available and are often part of extensive historic archives. Their lower resolution, on the other hand, inhibits studying urban morphology and change processes at a more detailed, intra-urban level. In this study, we develop spatial metrics for use on continuous sealed surface data produced by a sub-pixel classification of Landsat ETM+ imagery. The metrics characterise the shape of the cumulative frequency distribution of the estimated sub-pixel fractions within a building block by fitting an exponential and a sigmoid function with a least-squares approach. A classification tree is then used to relate the metric variables to urban land-use classes selected from the European MOLAND topology. This approach shows promising results, but still needs improvement which may be achieved by including spatially explicit metrics in the analysis.

I. INTRODUCTION

More than half of the world's population lives in urbanised areas, and in the future cities will house an increasing number of people in both absolute and relative terms [1]. While spatial expansion of cities is a natural consequence of demographic and economic trends and changes in lifestyle on which local and regional policy-makers have seemingly little grasp, local policy should be concerned about how population growth is translated into spatial patterns of urban growth. Urban sprawl and increased soil sealing provide symptomatic evidence for the fact that many European and North-American cities grow faster spatially than demographically. A study of the European Environment Agency confirms this by reporting that European cities have expanded on average by 78% since the mid-1950s, while during the same period the population increased by only

33% [2]. This dilution of the urban fabric has both direct and indirect impacts on the environment and the well-being of urban residents. For instance, uncontrolled sprawl increases energy consumption, pollution and greenhouse gas emissions, demands more transport infrastructure, may lead to increased flood risks and encroaches on natural landscapes. Effective urban management and planning strategies at different levels of government are therefore essential to temper the environmental consequences of urban land consumption. To develop and monitor such strategies and to assess their spatial impact, analysing and characterising changes in urban structure is of great consequence. Data from earth observation satellites provide regular information on urban development and could in that way contribute to mapping and monitoring structural characteristics of expanding cities. A rather novel approach in this research area is to describe urban form by means of spatial metrics, i.e. quantitative measures of spatial pattern and composition that have recently shown considerable potential for structural analysis of urban environments [3][4]. Spatial metrics derived from satellite imagery may also help to describe the morphological characteristics of urban areas and their changes through time [5]. Because previous studies have demonstrated a relationship between the spatial structure of the built-up environment and its functional characteristics [6], quantifications of urban morphology through spatial metrics can also be related to land-use. However, despite the currently available high resolution satellite images, which provide increasingly detailed information about urban surface materials, most of the historic archive imagery consists of medium resolution (MR) data such as from the Landsat or SPOT programmes. The lower resolution of such images often compels studies to treat cities as a single unit rather than to analyse them on an intra-urban basis. To study urban growth patterns with a time-span that exceeds the availability of high

2009 Urban Remote Sensing Joint Event

resolution imagery or in cases where data costs are of concern, spatial metrics that succeed in capturing structural information from images with a pixel size of 20 meters or more should be used. In this study, we aim to characterise urban structure and land use in the Greater Dublin area by developing spatial metrics for use on continuous sealed surface data produced by a sub-pixel classification of Landsat images. These spatial metrics are calculated for building blocks that are homogeneous in terms of land-use and will be used as variables by a classification tree, a well-known rule-based classifier, to allocate each building block to a particular land-use type. This approach will make it possible to tap into the extensive historic archives of MR images to characterise urban growth patterns at a reasonably detailed level, on an intra-urban basis and at low cost.

II. STUDY AREA AND DATA

The study area for this research is Dublin, the political and economical capital of Ireland and home to over 40% of the country's population. Dublin experienced rapid urban expansion in the 1980's and 1990's, fuelled by the building of new roads that drove residential and commercial development rapidly outward into the urban fringe. While the Greater Dublin area as a whole experienced only a moderate population growth of 3.6% between 1986 and 1996, population in the urban periphery increased more rapidly with as much as 9.6% in South Dublin and 21.1% in Fingal, to the north [7]. This has resulted in a hollowing of the central city and a simultaneous growth and movement into Dublin's low density, car-oriented and seemingly unplanned periphery [8]. A Landsat TM image (path 206, row 23) acquired on May 24th 2001 is used to derive spatial metrics for the study area. The image is geometrically co-registered to the Irish Grid projection system and the raw digital numbers are converted to exoatmospheric reflectance according to the formulas and calibration parameters presented by The Landsat 7 Users Handbook [9]. An existing land-cover map, derived from a Quickbird image acquired on August 4th 2003, is used to obtain reference data for training and validating the sub-pixel classifier. Reference land-use classes are acquired from the European MOLAND land-use typology¹

III. DERIVING CONTINUOUS SEALED SURFACE DATA

The downside of using MR data for urban analysis is the relatively low spatial resolution, which may lead to low mapping accuracies because the sensor's instantaneous field of view (IFOV) often contains different types of land cover, especially in urban areas. To overcome this drawback we applied sub-pixel classification, a technique that relates a pixel's spectrum to fractions of its surface constituents. One of the most common methods to approach this problem is linear spectral mixture analysis (LSMA), whereby a pixel's observed reflectance is modelled as a linear combination of spectrally pure "endmember" reflectances [10]. LSMA has recently received quite some attention in studies that aim to characterise

urban environments [11]. Some of these studies resort to the components of the Vegetation, Impervious surfaces and Soil (VIS) model proposed by [12] to represent the endmembers of the LSMA model. However, not all pure vegetation, man-made impervious surface or bare soil pixels necessarily occupy extreme positions in feature space and can, as such, not directly be used as endmembers for linear unmixing. One reason for this is that pure pixels are spectrally variable because of brightness differences, even though they may represent a similar surface type [13]. Another reason is spectral confusion between different land-cover types such as dry bare soils and bright impervious surfaces. While some studies on other areas did succeed in defining a soil endmember (e.g. [14]), this is not possible for the Dublin study area. We therefore opt to use a sub-pixel classification approach in which soil is not used as a separate surface component. Instead, a linear regression model is developed to estimate the proportion of vegetation cover within each Landsat pixel. Discounting for a moment the presence of water and exposed soil in cities, the vegetation fraction within a pixel can be considered as the complement of the man-made surface fraction. Temporal differences in vegetation cover between the ETM+ image and the reference samples taken from the high resolution land-cover map are filtered out by a temporal filtering technique based on iterative linear regression between NDVI values [15].

Because the regression model only estimates vegetation, and therefore does not explicitly distinguish urban from non-urban surface cover, a mask is developed to indicate pixels belonging to urban land cover. Only pixels within the urban mask are subjected to the unmixing model. To create this mask, we apply a non-parametric unsupervised classifier and enhance the output map with knowledge-based post-classification rules. The unsupervised classification approach is based on Kohonen self-organising maps (SOM) [16]. A SOM is a type of artificial neural network that was originally developed to visualise topologies and hierarchical structures of multi-dimensional data by transforming the input space into an ordered two dimensional map. The SOM architecture consists of two network layers: an input layer, which is fully connected to a typically two dimensional array of nodes called Kohonen layer or codebook vector map. A randomly initialised weight vector of the same dimension as the input data vectors is associated with each node. The SOM is trained by passing an input vector (i.e. a pixel's spectral values) to the network, and by choosing a winning node based on the smallest Euclidian distance between the input vector and the weight vectors. Then, the weights of the winning node and its neighbours are adjusted in order to reduce the node's distance to the input vector. After each image pixel or a representative set of image pixels is passed to the SOM during training, the built model can be applied to any part of the image and even to other images when atmospheric or other calibration constraints are taken into account. Because the trained SOM network assigns each pixel to a particular node in the codebook vector, each such node can be considered to represent a certain information category. This is similar to other unsupervised classification approaches, except that nodes or classes that are closer to each other on the codebook vector are also more spectrally similar, which makes them easier to interpret. In this research, we apply a SOM with

¹ MOLAND: Monitoring Land Use/Cover Dynamics. *MOLAND project website* URL: <http://www.moland.jrc.it>. Date last accessed: 12 March 2009

a 3 by 5 Kohonen layer, which divides the image into 15 spectral classes. Although Kohonen SOM is a rather advanced approach to unsupervised classification, spectral confusion between certain surface types is still likely to occur and will cause errors in the urban mask. To enhance the classification output with respect to the intended purpose, i.e. distinguishing urban from non-urban areas, a rule-based post-classification approach is adopted [17]. This method uses rules that operate on clumps or groups of adjacent pixels of the same class. If certain user defined criteria are met, a clump's original class label (O) is changed to a target class (T). For the purpose of developing an urban mask in this paper, the target class is always a neighbour's class label. Each rule uses two criteria: area (A) and adjacency (Ad). The area criterion constrains a rule's operation to clumps of a certain maximum size, expressed as number of pixels within the group. Adjacency constrains a rule to pixel groups that are next to clumps of a given type. The value of the adjacency criterion represents the fraction of the clump's border that is shared with the target class. For example: a rule might be developed to assign small bare soil groups (O = bare soil, A < 20 pixels) that share more than half of their border with urban clumps (Ad > 0.5) to the urban class (T). The values of O, T, Ad and A are determined from a visual inspection of the unsupervised classification, keeping in mind the intended use of the post-classification. For the purpose of developing an urban mask, it is especially important that confusion between rural bare soil and urban fabric is resolved, and that each class from the unsupervised classification is unambiguously assigned to either urban or non urban. In addition to the knowledge-based rules, all single pixel groups are removed from the map before and after post-classification to reduce the amount of noise. This is done by applying a majority filter on a 3 by 3 window centred on groups that consisted of only one pixel. The urban mask is validated by a visual sampling of about 1% of the image pixels (2897 pixels).

IV. CHARACTERISING URBAN STRUCTURE WITH SPATIAL METRICS

A. Defining the spatial domain

Spatial metrics are calculated within a spatial domain, i.e. a relatively homogeneous spatial entity that represents a basic landscape element. Naturally, the definition of the spatial domain directly influences the metrics and will depend on the aims of the study and the characteristics of the landscape [3]. Some studies conduct global comparative analyses of urban form and define an entire city as a single spatial domain [18]. Other studies examine intra-urban growth patterns or land-use changes at a coarse level and divide the urban landscape into relatively large administrative zones (e.g. [5]), concentric buffer zones [19] or large rectangular sample plots [20]. If an analysis of urban morphologies, land-use or change processes is required at a spatially more detailed intra-urban level, the city has to be divided up into smaller and relatively homogeneous units [5]. A commonly used approach in remote sensing data analysis is the use of a moving window or kernel, from which statistical or structural information can be derived. Kernel-based methods, however, have a number of

disadvantages compared to region-based approaches, including the difficulty of selecting an optimal kernel size and the fact that the kernel is an artificial construct that does not conform to real urban land-use zones or morphological units [6]. In this study, we define the spatial domain by intersecting a detailed road network with the MOLAND land-use map. This provides us with 5767 blocks that are relatively homogeneous in terms of land-use.

B. Spatial metrics based on the cumulative frequency distribution of sealed surfaces

The hypothesis of our research is that the composition of the building blocks in terms of the distribution of the sub-pixel sealed surface proportions provides an indication of the land-use class to which it belongs. As a first step, the percentage of sealed surfaces within each block is calculated. The blocks are then divided into 4 classes according to their degree of soil sealing: 0-10%, 10-50%, 50-80% and more than 80%. The definition of these four classes is based on the criteria used in the MOLAND scheme to distinguish continuous from discontinuous urban fabric and residential discontinuous urban fabric from residential discontinuous sparse urban fabric. This provides us with a map that is used to stratify the study area: blocks with less than 10% sealed surfaces are labelled as non-urban land (fallow land, large vegetated areas, sea, etc.) and blocks with more than 80% sealed surface cover as continuous, dense urban fabric. The remaining 3494 blocks with 10-80% sealed surface cover are subjected to an analysis with spatial metrics because they belong to different land-use types such as sparse residential areas versus industrial zones with empty, vegetated plots and commercial or service areas. These land-use types cannot be distinguished based only on the average sealed surface cover.

To further characterise our building blocks, the cumulative frequency distribution (CFD) of the proportion sealed surface cover of the Landsat pixels is examined. We assume that the shape of this distribution function can be related to the morphological characteristics and hence the land-use type of the building block it represents. Low and medium mixed residential land-use blocks, for instance, contain more mixed urban-vegetation pixels than industrial areas, which is reflected by a sigmoid-shaped CFD. To express the CFD's shape quantitatively, two functions are fitted using a least-squares approach:

$$P(x) = \frac{a}{b + e^{-cf}} + d \quad (1)$$

and

$$P(x) = a.b^f. \quad (2)$$

Where P(x) is the predicted cumulative frequency within block x of impervious surface fraction f and a, b, c and d are function parameters determined by the least-square approach. Function (1) can assume an S-shape, which is suitable to represent residential areas, while (2) is an exponential function, more suited to represent industrial zones and other types of non-residential land. The error of fit E(x) can be expressed as:

$$E(x) = |P(x) - CFD(x)| \quad (3)$$

where $CFD(x)$ is the observed cumulative frequency distribution of block x . The parameters of these functions are used as spatial metrics to describe the morphology of the land-use blocks. The errors of fit for functions (1) and (2) and the difference between them are also included as variables because they too provide an indication of which function best describes the CFD of a building block. The area of the blocks in square meters and the average sealed surface proportion are used as non-CFD based metrics.

C. Setting the rules with a classification tree

To examine the CFD based metrics and link them to the MOLAND land-use classes, a supervised classification based on classification trees is applied. Classification tree analysis is a well known data mining technique used to predict or explain responses of cases on a categorical, dependent variable from scores on independent, predictor variables [21]. It is a transparent and useful exploratory technique to objectively define thresholds on the CFD-based spatial metrics and to derive sets of rules that assign each building block with a sealed surface cover between 10 and 80% to an urban land-use class. To train the classifier, a random learning sample of 100 cases for each of 5 land-use classes is selected: residential (1), industrial (2) and commercial areas (3), public and private services (4) and recreation, sports and green urban zones (5). A classification tree can perfectly describe any data set if enough rules are defined, so in order to avoid over-fitting, the tree is pruned to restrict its size to a comprehensible set of about 15 rules. The classifier is then applied to all building blocks with 10-80% sealed surface cover. Its performance is assessed by comparing the predicted class memberships to the MOLAND land-use map, taking into account the size of the building blocks. This is achieved by putting an area based weight on each block in the error calculation. The reasoning behind this weighting is that misclassifying small blocks is less severe than misclassifying large blocks in the final predicted land-use map.

V. RESULTS AND DISCUSSION

The accuracy of the vegetation proportions predicted by the regression model (table I) is assessed with a temporally filtered validation sample that consists of 2500 ETM+ pixels, for which the reference proportions are determined from down sampling the land-cover classification derived from a Quickbird image. The mean absolute error (MAE) is an indication of the error magnitude. It tells us that, on average, an error of 0.10 (or 10%) is made in the estimation of the vegetation fraction within each pixel. The mean error (ME) on the other hand represents the error bias. Its value close to zero indicates that overestimations compensate underestimations within the sample. From the standard deviations (σ) we can learn that 95% of the over and underestimations fall within the interval of -0.27 to 0.28.

TABLE I. ESTIMATION ERRORS OF VEGETATION FRACTION

MAE	ME	RMSE	σ (MAE)	σ (ME)
0.105	0.005	0.141	0.095	0.141

The sub-pixel sealed surface fractions are considered the complement of the estimated vegetation fractions within the ETM+ pixels labelled as urban by the unsupervised, SOM based land-cover classification of the ETM+ image. The 15 initial classes of the land-cover map produced by the SOM classifier are recoded into 6 meaningful information classes (fig. 1a). The map shows a high level of spectral confusion between urban, bare soil and one of the vegetation classes, which makes it impossible to directly use the classification output as an urban mask. To enhance the unsupervised classification output, three knowledge-based post-classification rules (table II) are developed and applied in combination with a filter to remove individual, isolated pixels. The first rule re-assigns erroneous bare soil clumps within the urban fabric to neighbouring urban type clumps. The adjacency threshold is set to a relatively high 0.75, meaning that bare soil clumps that share at least 75% of their border with an urban clump have their class changed to urban. Because actual fallow fields do not share a large part of their border with urban surfaces, setting an area threshold is not necessary. This rule effectively cleans up most of the bare soil/urban confusion in the city centre. The high degree of confusion in the classification produces some larger misclassified areas near the western part of the city, which the post-classification is not able to fully resolve. A few large misclassified clumps are therefore manually corrected after visual inspection. A second post-classification rule is developed to operate on parts of low density urban areas that were classified into the same class as peat and bog, a type of vegetation cover that is common in the Wicklow Mountains. Because all misclassified clumps of this type within the city are relatively small compared to actual peat and bog regions, an area threshold is sufficient to improve the classification. A third and final rule is applied to remove small groups of shadow pixels in the city. To avoid confusion with shadows near vegetation, an adjacency threshold is used together with the area threshold.

TABLE II. KNOWLEDGE-BASED POST-CLASSIFICATION RULES

Rule	Original class	Target class	Area	Adjacency
1	Bare Soil	Urban	Unlimited	0.75
2	Mixed urban-vegetation	Urban	< 200	Unlimited
3	Shadow	Urban	< 1000	0.75

After post-classification, the land-cover map clearly improves (fig. 1b). The overall accuracy and the kappa index of agreement derived from the confusion matrix of the validation sample are 93% and 89% respectively. The highest errors are found for the bare soil class, which has a producer's accuracy of 68% and a user's accuracy of 88%. This error is caused for a large part by confusion between bare soil and vegetation,

2009 Urban Remote Sensing Joint Event

which can be attributed to the mixed pixel problem (e.g. agricultural fields and pastures). Another explanation is misclassification among bare soil and urban areas, which is due to spectral similarities, especially within the numerous construction zones within the area.

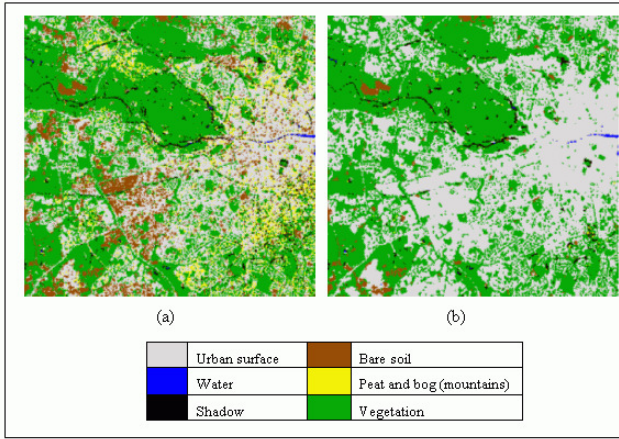


Figure 1. Land-cover classification created by self-organising map (a) and enhancement by knowledge-based post-classification (b).

From a combination of the urban mask and the complement of the vegetation proportions estimated by linear regression, a sealed surface map of the study area can be produced (fig. 2). This map forms the basis for deriving spatial metrics. The average sealed surface cover for each of the building blocks can also be calculated from it. This is useful to visualise the built-up density within the study area (fig. 3). The built-up density map clearly shows the urban gradient: from a compact and dense city centre to a low density, sprawled sub-urban zone.

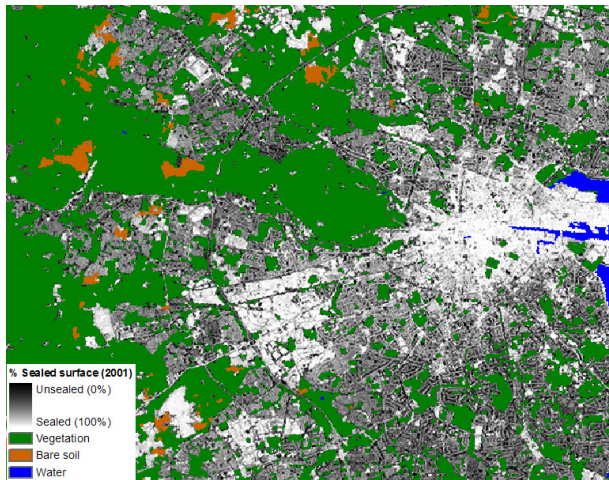


Figure 2. Combination of urban mask and estimated sealed surface cover for part of the Dublin study area.

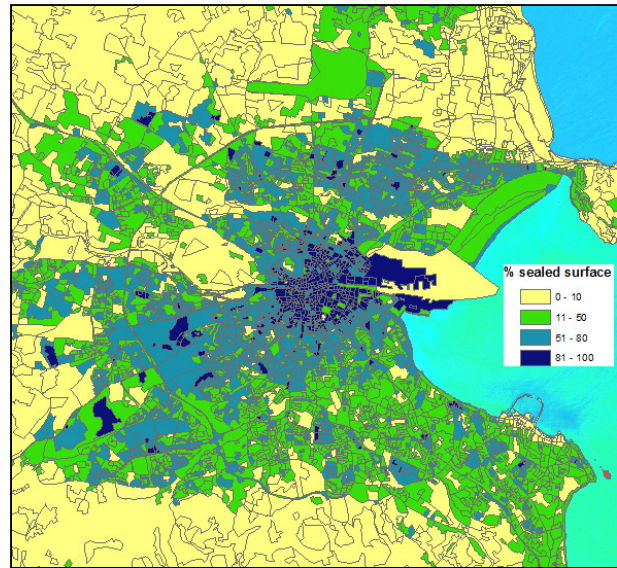


Figure 3. Urban density map based on average sealed surface cover within building blocks.

To further characterise the building blocks, functions (1) and (2) are fitted to the cumulative frequency distribution of each block. Figs. 4 and 5 show typical examples for blocks with industrial and residential land-use. For industrial land-use (fig. 4), the CFD takes an exponential form, which results in a relatively low fitting error for the exponential function. For residential land-use (fig. 5), the CFD is S-shaped and consequently the error of fit of the exponential function is much higher. The difference in error of fit between the industrial and residential land-use types can be exploited to distinguish them in an automated approach. The shape of the fitted functions, such as the steepness of the sigmoid curve, is reflected by the function parameters and may also represent discriminatory information.

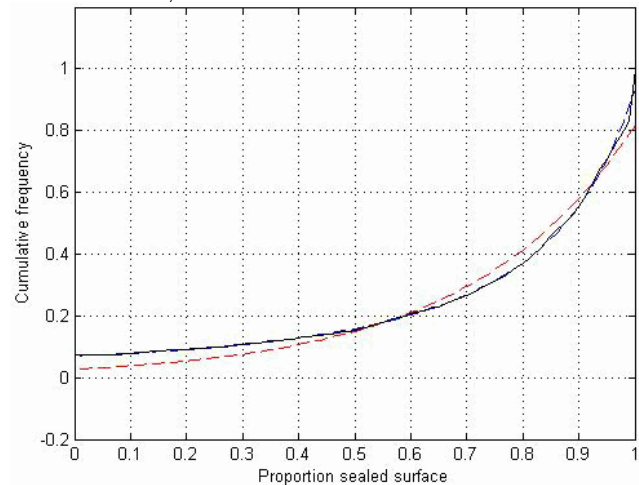


Figure 4. Cumulative frequency distribution of building block with industrial land-use type. Error of fit of sigmoid function (blue) = 0.37, of exponential function (red) = 2.91

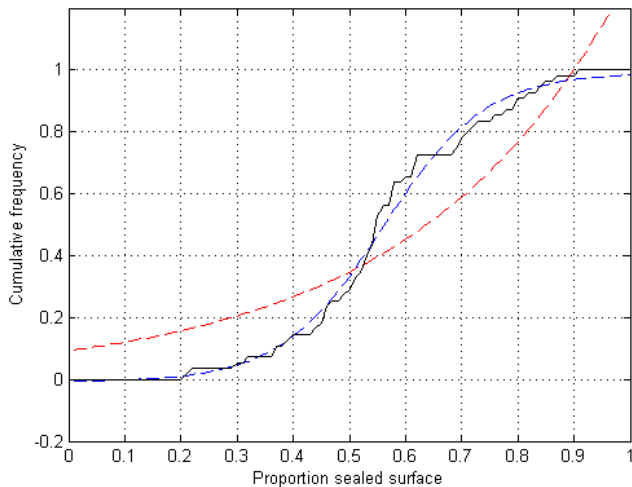


Figure 5. Cumulative frequency distribution of building block with residential land-use type. Error of fit of sigmoid function (blue) = 2.09, of exponential function (red) = 13.6

To relate the parameters of the fitted functions to the 5 urban land-use types of blocks with 10%-80% sealed surface cover, a classification tree is developed using the learning sample of 100 blocks per class. The resulting, pruned tree has 16 rules, most of which apply a combination of the error of fit of the exponential function, the parameters of the sigmoid function, the sealed surface cover and the size of the block. The overall error of 78%, weighted according to the size of the building blocks (table III), is acceptable but hides the poor performance of the classifier for commercial areas and services because these land-use types are less prominent in the study area. The cause of this low accuracy lies in the confusion with residential land, and in the confusion among the two classes themselves. The classifier also confuses services with industrial areas in some cases, which explains the mediocre user's accuracy of 65% for this class. A quarter of the blocks with sports and recreation facilities is labelled as services because many public or private services in our study area are also situated in green areas. On the other hand, quite some sparsely built residential blocks are recognised as green areas, which accounts for the relatively low user's accuracy of the recreation, sports and green urban class. The low accuracies for the non-residential land-use types may indicate that the cumulative frequency distribution in itself is not sufficient to fully capture the information provided by the sealed surface fractions within the building blocks. This may be explained by the fact that the frequency distribution only represents information about the composition of the pixels and not about their spatial positioning and structure. If only a distinction is made between residential and non-residential land, the overall accuracy increases to 86% and the per-class errors are at an acceptable level.

TABLE III. AREA WEIGHTED ACCURACIES OF 5 MAIN URBAN LAND-USE TYPES OF BUILDING BLOCKS WITH 10-80% SEALED SURFACE COVER

Land-use class	UA	PA	UA	PA
Residential	0.95	0.83	0.95	0.83
Industrial	0.65	0.82	0.73	0.92
Commercial	0.22	0.40		
Services	0.37	0.38		
Recreation,sports and green urban	0.58	0.75		
Overall error	0.78		0.86	

VI. CONCLUSIONS

In this research, the cumulative frequency distribution of sealed surface proportions derived from a sub-pixel classification of Landsat ETM+ pixels was used to characterise urban morphology within building blocks. The shape of the frequency distribution was quantified by parameters of fitted functions, constituting a type of spatial metric that exploits the advantages of continuous land-cover data, which in turn can be obtained from medium resolution satellite imagery. This approach showed promising results when it was applied to distinguish general land-use types such as residential versus non-residential land. In combination with building block density information derived from the sealed surface map, it is possible to define different residential morphologies. A further distinction among functional land-use types such as commercial land and services was less successful. For that purpose, metrics that exploit the spatial relationships of the continuous sealed surface data within the building blocks may be required. This is a topic for further research.

ACKNOWLEDGMENT

The research presented in this paper was supported by the Belgian Science Policy Office in the frame of the STEREO II programme - project SR/00/105.

REFERENCES

- [1] G. Martine, *The State of the World Population 2007*. New York: United Nations Population Fund, 2008.
- [2] European Environment Agency (EAA), *Urban Sprawl in Europe – the Ignored Challenge*. Brussels: OPEC, EAA report 10, 2006.
- [3] M. Herold, H. Couclelis, and K.C. Clarke, "The role of spatial metrics in the analysis and modelling of urban land use change," *Comput. Environ. Urban*, vol. 29, pp. 369-399, 2005
- [4] P.M. Torrens, "A toolkit for measuring sprawl," *Applied Spatial Analysis*, vol. 1, pp. 5-36, 2008
- [5] W. Ji, J. Ma, R.W. Twibell, and K. Underhill, "Characterising urban sprawl using multi-stage remote sensing images and landscape metrics," *Comput. Environ. Urban*, vol. 30, pp. 861-879, 2006.
- [6] S. Barr and M. Barnsley, "A region-based, graph-theoretic data model for the inference of second-order thematic information from remotely sensed images," *Int. J. Geogr. Inf. Sci.*, vol. 11, pp. 555-576, 1997.
- [7] P. Kitchen, "Identifying changes of urban social change in Dublin – 1986 to 1996," *Irish Geogr.*, vol 35, pp. 156-174, 2002.

2009 Urban Remote Sensing Joint Event

- [8] M.J. Bannon, "The Greater Dublin Region: planning for its transformation and development," in *Dublin: Contemporary Trends and Issues for the Twenty-first Century*, J. Killen and A. MacLaran, Eds. Dublin: Geographical Society of Ireland, 1999, pp. 1-19.
- [9] R.R. Irish, *Landsat 7 Science Data Users Handbook*. Greenbelt, MD: NASA, 2007.
- [10] F. van der Meer, "Image classification through spectral unmixing," in: *Spatial Statistics for Remote Sensing*, A. Stein, F. van der Meer, and B. Gorte, Eds. Dordrecht: Kluwer Academic Publishers, 1999, pp. 185-193.
- [11] T. Rashed, J.R. Weeks, D. Stow, and D. Fugate, "Measuring temporal composition of urban morphology through spectral mixture analysis: towards a soft approach of change analysis in crowded cities," *Int. J. Remote Sens.*, vol 26, pp. 699-718, 2005.
- [12] M.K. Ridd, "Exploring a V-I-S (Vegetation-Impervious Surface-Soil) model for urban ecosystem analysis through remote sensing - Comparative anatomy for cities," *Int. J. Remote Sens.*, vol. 16, pp. 2165-2185, 1995.
- [13] C. Wu, "Normalized spectral mixture analysis for monitoring urban composition using ETM+ imagery," *Remote Sens. Environ.*, vol. 93, pp. 480-492, 2004.
- [14] S. Phinn, M. Stanford, P. Scarth, A.T. Murray and P.T. Shyy, "Monitoring the composition of urban environments based on the vegetation-impervious-soil (VIS) model by subpixel analysis techniques," *Int. J. Remote Sens.*, vol. 23, pp. 4131-4153, 2002.
- [15] T. Van de Voorde, T. De Rooeck and F. Canters, "A comparison of two spectral mixture modelling approaches for impervious surface mapping in urban areas," *Int. J. Remote Sens.*, in press.
- [16] T. Kohonen, *Self-Organizing Maps*, 3rd ed. Berlin: Springer, 2001.
- [17] T. Van de Voorde, W. De Genst, and F. Canters, "Improving pixel-based VHR land-cover classifications of urban areas with post-classification techniques," *Photogramm. Eng. Remote Sens.*, vol. 73, pp. 1017-1027, 2007.
- [18] J. Huang, X.X. Lu, and J.M. Sellers, "A global comparative analysis of urban form: applying spatial metrics and remote sensing," *Landscape Urban Plan.*, vol. 82, pp. 184-197, 2007.
- [19] K. C. Seto and M. Fragkias, "Quantifying spatiotemporal patterns of urban land-use change in four cities of China with time series landscape metrics," *Landscape Ecol.*, vol. 20, pp. 871-888, 2005.
- [20] Y.C. Weng, "Spatiotemporal changes of landscape pattern in response to urbanization," *Landscape Urban Plan.*, vol. 81, pp. 341-353, 2007.
- [21] L. Breiman, J.H. Friedman, R.A. Olshen, and C.J. Stone, *Classification and Regression Trees*. Belmont, CA: Wadsworth International Group, 1984.